AGU100 ADVANCING EARTH AND SPACE SCIENCE

Geophysical Research Letters

RESEARCH LETTER
10.1029/2019GL084473

The Vertical Distribution of the Optical Emissions of a Steve and Picket Fence Event

W. E. Archer[1], J.-P. St.- Maurice[1,2], B. Gallardo-Lacourt[3], G. W. Perry[4], C. M. Cully[5], E. Donovan[5], D. M. Gillies[5], R. Downie[6], J. Smith[6], and D. Eurich[6]

[1]Department of Physics and Engineering Physics, University of Saskatchewan, Saskatoon, Saskatchewan, Canada, [2]Department of Physics and Astronomy, University of Western Ontario, London, Ontario, Canada, [3]NASA/GSFC, Greenbelt, MD, USA, [4]Center for Solar-Terrestrial Research, New Jersey Institute of Technology, Newark, NJ, USA, [5]Department of Physics and Astronomy, University of Calgary, Calgary, Alberta, Canada, [6]Alberta Aurora Chasers, Calgary, Alberta, Canada

Key Points:
- The optical emissions of Steve range from 130 to 270 km in altitude
- The optical emissions of the green Picket Fence range from 95 to 150 km in altitude
- Steve and the Picket Fence extend vertically along similar magnetic field lines

Supporting Information:
- Supporting Information S1

Correspondence to:
W. E. Archer,
wea784@usask.ca

Citation:
Archer, W. E., St.-Maurice, J.-P., Gallardo-Lacourt, B., Perry, G. W., Cully, C. M., & Donovan, E. et al. (2019). The vertical distribution of the optical emissions of a Steve and Picket Fence event. *Geophysical Research Letters*, *46*, 10,719–10,725. https://doi.org/10.1029/2019GL084473

Received 8 JUL 2019
Accepted 29 AUG 2019
Accepted article online 3 SEP 2019
Published online 11 OCT 2019

Abstract So-called "Steve" subauroral purple emissions have recently been uncovered by auroral photographers and have rapidly become an intense subject of debate as to their origin. In some events, nearby periodic green emissions have also been uncovered and given the name "picket fence," owing to their appearance. The present paper advances our understanding of these phenomena by narrowing down the altitude extent of the Steve and picket fence emissions. Our determination is based on the event of 16 September 2017, which was simultaneously observed from two vantage points, allowing for a determination of the height range of Steve and picket fence through triangulation. We show that the picket fence extend between 95- and 150-km altitude and is aligned with the geomagnetic field, while the Steve altitude spread is between 130 and 270 km. We also show the two phenomena to be on nearby or perhaps the same magnetic field lines.

1. Introduction

The scientific community has recently reported on a nighttime optical phenomenon called Steve. Steve is described as a purple band of light observed equatorward of aurora, spanning only tens of kilometers in latitude but thousands of kilometers in longitude (Gallardo-Lacourt, Nishimura, et al., 2018). Archer et al. (2019) were able to find eight occurrences of Steve with near-coincident satellite measurements, and they show Steve to be consistently associated with intense subauroral ion drifts (SAID). The notion of Steve as an optical signature of SAID was put forward by MacDonald et al. (2018). Typical of SAID, these events were near the ionospheric projection of the plasmapause, with either near-zero or downward field-aligned current, which suggests that Steve is not caused by precipitating electrons. Particle measurements from the Polar Operational Environmental Satellites coincident with an occurrence of Steve shows there is insufficient particle precipitation to cause the optical signature of the phenomenon (Gallardo-Lacourt, Liang, et al., 2018). These studies suggest that Steve may be related to the plasma heating present in very intense SAID.

Steve is at times accompanied by green bands of light called the "picket fence." It is currently unknown if these two phenomena are causally linked. While Steve has been reported on several occasions in the absences of the picket fence, the picket fence has not yet been reported in isolation. Nishimura et al. (2019) presented measurements from the Defense Meteorological Satellite Program coincident with two different Steve events, one with picket fence and one without. They report a region of kiloelectron volts precipitating particles roughly coincident with the event including a picket fence, detached from the auroral oval. Based on these observations, Nishimura et al. (2019) suggest that while plasma heating may contribute to Steve, the picket fence seems to be caused by precipitating electrons.

Recent spectral measurements of the picket fence presented by Gillies et al. (2019) are also consistent with the phenomena being caused by precipitating electrons, as they show the picket fence to be dominated by OI 557.7-nm emissions. Gillies et al. (2019) also show that the spectral observations of Steve have two major contributing components: OI red-line emissions and a continuous spectral enhancement spanning approximately 400–730 nm. The red emissions could be caused by soft electron precipitation, except for the fact that, as previously stated, Steve does not appear to be coincident with precipitating particles. Alternatively, red emissions could result from the recombination of molecular oxygen as occurs in polar-cap patches

(Weber et al., 1984; Weber et al., 1986). Another possibility would be impact from hot thermal electron as occurs in stable red arcs (Cole, 1965; Kozyra et al., 1990). However, none of these mechanisms explain the purple appearance of Steve which, based on the work of Gillies et al. (2019), is due to a continuum visual spectrum. In many of these previous studies, the name "Steve" was presented as the acronym for Strong Thermal Emission Velocity Enhancement. As the physical mechanisms responsible for this phenomenon have not yet been established, in this study we will simply refer to it as Steve.

In order to further constrain the physical mechanisms that could be responsible for Steve and the picket fence, we have sought to determine the altitude range of the phenomena. Altitude estimates of Steve in previous studies (Archer et al., 2019; MacDonald et al., 2018) have been based on the presence of the atomic oxygen red-line emissions inside Steve, resulting in estimates around 230 km, as is typical for red-line emissions (Gillies et al., 2017). In the present study we have converged on one occurrence of the Steve and picket fence phenomena that took place from approximately 5–6 UT on 16 September 2017. Although no scientific ground-based optical measurements were taken of this event due to its location (south or west of the field-of-view of all-sky cameras), dozens of amateur auroral photographers captured Steve from western Alberta and eastern British Columbia. By comparing two simultaneous observations that were taken hundreds of kilometers apart in the north-south direction, we have narrowed down the altitude ranges and latitude of the two phenomena. We have also found that the observations are consistent with Steve and the picket fence being essentially on the same magnetic field lines.

2. Methodology

In order to interpret photographic observations of Steve, we first had to establish a coordinate system within each photograph. To do so, we relied on the background star field in each photograph. With the location and time of each photograph in hand, the azimuth and elevation angle of any given star in the night sky could be determined. From that information, we could in turn determine the exact angular position of the boundaries of the Steve and picket fence structures.

Most photographs of Steve are taken with a 20-s integration period. As a result, even stars with apparent magnitudes greater than 8 are clearly visible (the faintest stars visible by the unaided human eye have apparent magnitudes around 6.5). We identified stars using the "SkySafari" (2019) application and tabulated their azimuths and elevations from the "StarData" function available in Mathematica (2017). We could not establish a linear coordinate system over an entire image because the field of view of cameras is not flat. We defined the boundary of optical features by their brightness, the edge of the features being 50% of the peak emission intensity. The upper boundary of the picket fence cannot be identified with this boundary definition because the background (Steve) is too bright. For the upper boundaries of the picket fence, we instead qualitatively identified the region where the green of the picket fence transitioned into the white of Steve. We then identified stars angularly colocated with boundaries of optical features in order to directly measure the angular location of those optical features. Two examples of this are shown in Figure 1. Stars angularly colocated with the edge of Steve are marked with empty squares and triangles, while those colocated with the end of a picket fence are marked with filled squares and triangles. Squares mark the top or southern boundary of optical features (depending on the observers perspective), while triangles mark the bottom or northern boundary. Once we identified the angular positions of interest, we mapped them out into geodetic space using the aer2geodetic submodule within the pymap3d module for python (Hirsch, 2016).

The photograph in Figure 1a was taken by Robert Downie, who we will call Observer 1 (O1), at approximately 05:53:14 UT looking south from the campground near Berg Lake (53.1534° N, 119.1538° W, 1,680-m altitude). O1 took 109 photographs of Steve between 05:00 and 06:05 UT. This large number of photographs made it an ideal data set for comparison with photographs from other observers as it is likely that a temporally coincident photograph was taken. O1 was roughly 250 km north of Steve, so that, ideally, to minimize uncertainty in triangulation, a second observer should be located directly beneath Steve. One such photograph was obtained and is shown in Figure 1b. It was taken by Janis Smith (O2) from the shores of Shushwap Lake (50.9666° N, 119.3541° W, 530-m altitude). The location of O1, O2, and a third photographer named Dale Eurich (O3) are shown in Figure 1c along with the rough location of a portion of Steve accessed by the photographs and which has been shaded purple in Figure 1c.

To verify the time stamp of O1's photographs, we identified a star angularly colocated with the eastern peak of Mount Robson (53.1155° N, 119.1688° W, 3,400-m altitude). The star HD 206739 is highlighted in red

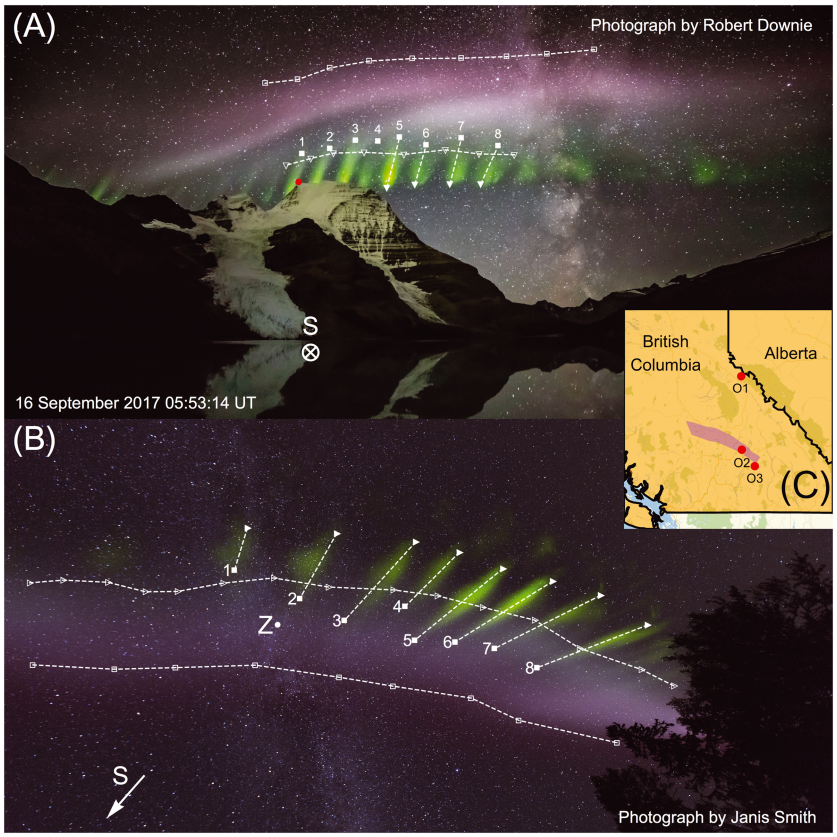

Figure 1. (a) Photograph of Steve taken around 05:53 UT on 16 September 2017 by Robert Downie (O1). The southward direction is labeled with S. Stars angularly colocated with the top and bottom edge Steve are marked with empty squares and triangles, respectively. Stars angularly colocated with the top and bottom of the picket fences are marked with filled squares and triangles, respectively. The star HD 206739, which is angularly colocated with the eastern edge of the top of Mount Robson, is marked with a red dot. (b) Photograph of Steve taken around 05:53 UT on 16 September 2017 by Janis Smith (O2). The southward and zenith directions are labeled with S and Z, respectively. Stars angularly colocated with the southern and northern edges of Steve are marked with empty squares and triangles, respectively. Stars angularly colocated with the southern and northern edges of the picket fences are marked with filled squares and triangles, respectively. In both (a) and (b), the picket fence structures are enumerated for reference. (c) The position of O1, O2, and Dale Eurich (O3) are shown along with a rough estimate of the location of a portion Steve.

in Figure 1a and had a position of 178.3° azimuth, 25.1° elevation from O1's position at the recorded time of the photograph. This is within 1° of the expected location of the eastern peak of Mount Robson (178.2° azimuth, 24.3° elevation) and confirms O1's time stamp to be accurate to within 1 min. The time stamps of O2's photographs could not be relied on. We therefore identified a photograph by O1 that was most likely to be coincident with O2's photograph by comparing the optical structures recorded by the two observers. O2 took four photographs of Steve over a period of 28 min. By comparing the temporal evolution of Steve reported by O2 and O1, we determined that the photograph shown in Figure 1b was taken between 05:50 and 05:55 UT. We then further refined our time determination by mapping out the angular position of the picket fence structure reported by the two observers. The latter was steadily moving westward (at between 200 and 300 m/s), and we identified the O1 photograph shown in Figure 1a to be the image most likely to coincide with O2's photograph. During this period of time, O1 took a photograph every 20 s. As such, we know the relative timing of O1 and O2's photographs to within 20 s. Assuming a time stamp of 05:53:14 UT for O2's photograph, her picket fence observations mapped into geodetic coordinates pass within 2 km horizontally of O1's photograph. Also note that both observers reported the fourth picket when counting east to west to be shorter than either of its neighbors.

Having identified the most likely time at which O2's photograph was taken, we estimated the altitude of Steve and the picket fence based on the photographs shown in Figure 1. For the picket fence, this was done by mapping out the altitude and azimuth of the top and bottom of each green picket from both perspectives

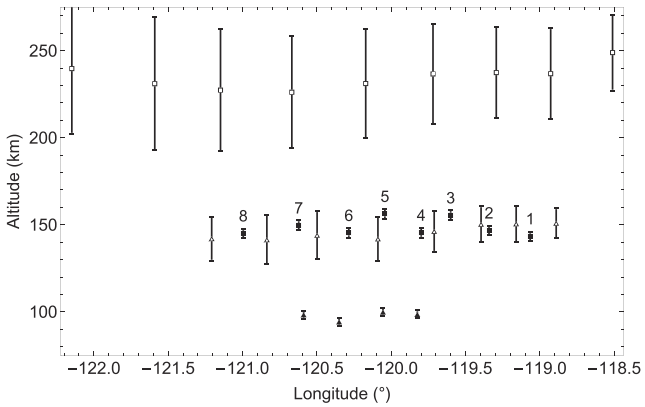

Figure 2. Most likely altitudes and longitudes of the boundaries of Steve and the picket fence identified in Figure 1a. The top and bottom of Steve are marked with empty squares and triangles, respectively. The top and bottom of the picket fence are marked with filled squares and triangles, respectively. The picket fence structures are enumerated in the same fashion as in Figure 1a for reference.

and identifying the point at which the two rays (nearly) intersected. For example, the top of the westmost picket that is marked with an filled square in Figure 1 is angularly coincident with the star HD 185762 from O1's perspective, which was at 214.85° azimuth and 31.35° elevation from O1's position at time of the photographs in Figure 1. From O2's position the top of that same green picket was angularly coincident with HD 156629, which was at 297.67° azimuth and 51.00° elevation. Each of these angles define a ray pointing away from their observer. These rays nearly intersect (their closest point separated by 0.5 km) around 51.49° N, 121.00° W, at 145-km altitude.

A comparison of pairs of rays was not possible for Steve as it is lacks sufficient structure to identify common features between the two observers. Instead, the boundaries of Steve identified in O2's photograph were used to define two surfaces: the northward and southward boundaries of Steve. In contrast, the stars identified in O1's photograph mark the upper and lower boundaries of Steve. We then estimated the altitude range of Steve by calculating the positions at which the upper and lower rays passed through the northward and southward boundaries of Steve. For example, the westmost bottom edge of Steve marked with a empty triangle in Figure 1a is angularly coincident with the star HD 183369 from O1's perspective, which was at 217.62° azimuth and 29.63° elevation from O1's position at time of the photographs in Figure 1. Starting from O1's position, this ray crossed the northern boundary of Steve (as defined by O2's photograph) at 51.62° N, 121.04° W, at 129-km altitude and crossed the southern boundary of Steve at 51.3251° N, 121.376° W, at 155-km altitude. The average of these two positions results in an altitude estimate of 142 ± 13 km.

3. Results

Based on the methodology described in the previous section and as shown through Figure 2, our estimates for the altitude of the bottoms of the pickets range is between 92 and 97 km while the tops are from 141- to 153-km altitude. Note that the uncertainty in the individual altitude determination is less than the variation in the mean altitude. The dominant source of uncertainty stems from the uncertainty of the pickets' precise location, owing to their inherent thickness, which is approximately 5 km. We propagated this 5-km uncertainty in the meridional position of the picket fence through the triangulation calculations described above, which results in an altitude uncertainty of roughly 2 km. The altitude uncertainty caused by the 1-min uncertainty in the timing of the photographs is less than 100 m and is negligible. We note that the pickets shown in Figure 2 are horizontally separated from one another by between 15 and 25 km, with an average spacing of 18 km.

Our estimates of the lowest boundary of Steve range from 141 to 151 km. The estimates for its upper boundary range from 226 to 249 km. Due to the meridional thickness of Steve from O2's perspective, there is a 20-km uncertainty in the meridional location of the bottom of Steve and a 35-km uncertainty in the meridional location of the top of Steve. When we propagate these meridional uncertainties through our triangulation calculations, our altitude estimates have uncertainties in altitude of roughly 15 km for the lower boundary and 30 km for the upper boundary of Steve.

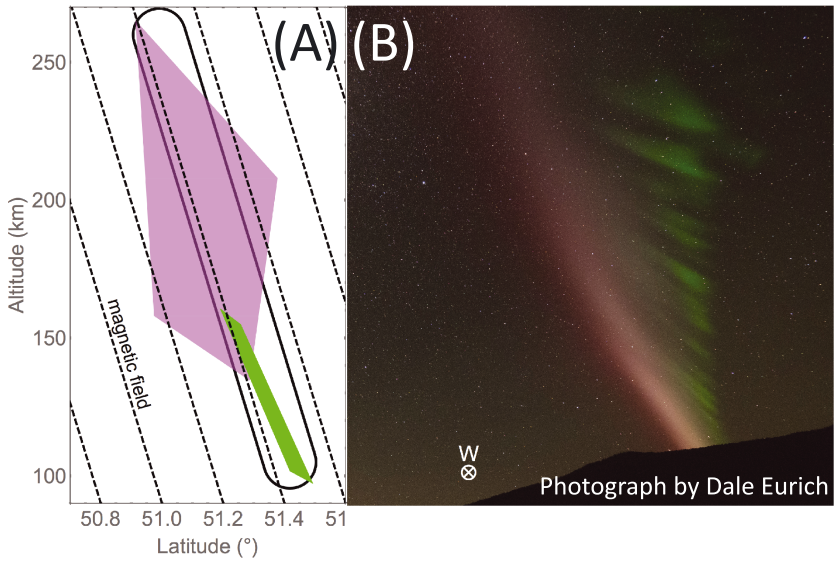

Figure 3. (a) In purple quadrilateral, area within which Steve has to be located, based on the triangulation of photographs shown in Figure 1. In narrow green quadrilateral, estimated boundaries of the picket fence. (dashed lines) Projection of the local magnetic field. (closed black contour) Possible overall area over which Steve and the picket fence would overlap through common magnetic field lines. (b) A westward facing photograph of Steve taken around 05:44 UT on 16 September 2017 by Dale Eurich (O3). Westward direction labeled with W.

The source of the more considerable uncertainties in the altitude estimates of Steve is better understood when observations are plotted in latitude and altitude, as shown in Figure 3a. The purple quadrilateral shown in this figure marks the region within which we estimate Steve to be. As O1 simply provides an upper and lower boundaries and O2 provides a northward and southward boundaries for the phenomenon, all we can ascertain is that Steve is within this quadrilateral. The size of the quadrilaterals in Figure 3 represent the uncertainty in the position triangulation of Steve and the picket fence. However, quite remarkably, we note that in Figure 3a, the upper-southern corner of the purple quadrilateral, the lower-northern corner of the quadrilateral, and the estimated location of the picket fence (shown in green) are all basically aligned and that the angle of that line is consistent with the angle of the Earth's magnetic field at the location of the observations, as shown as a series of black dashed lines in Figure 3. It is a sensible assumption that the green pickets each roughly trace the Earth's magnetic field as they appear to be caused by precipitating electrons. The precise alignment of Steve and the picket is difficult to discern because of the significant uncertainty in the location of Steve. However, Figure 3 shows that Steve and the picket fence are within 0.3° (35-km separation) of each other. In Figure 3b, we show a photograph by O3 of the Steve event looking westward around 05:44 UT, roughly 10 min prior to the photographs shown in Figure 1. As this photograph was not taken at the same time as the others, it does not directly improve our triangulation of Steve or the picket fence. However, it provides a different observation angle than the other photographs and is qualitatively consistent with Steve and the picket fence extending up and southward along similar magnetic field lines.

We can estimate the altitude range of Steve far more precisely under the assumption that it extends along the Earth's magnetic field. Under this assumption, O2's northward boundary of Steve corresponds to O1's lower boundary, and O2's southward boundary corresponds to O1's upper boundary. The results of this calculation are shown as an axis superimposed on a portion of O1's photograph, shown in Figure 4a. The additional constraint of the Earth's magnetic field does not change the estimated altitude for the picket fence but extends the altitude range of Steve to between roughly 130 and 270 km with faint emissions visible up to 300 km. The dominant source of uncertainty for the altitude estimates shown in Figure 4 stems from the fuzzy boundary of Steve which results in an uncertainty in altitude of approximately 2 km, similar to the uncertainty in the altitude of the picket fence discussed above. We separated the red, green, and blue channels for each pixel in the photograph shown in Figure 4a and show the median brightness of those channels for each row of pixels in Figure 4b. The *y* axis of this figure is scaled to match the pixel rows in Figure 4a. We note that the picket fence is seen primarily in the green channel of the photograph, while Steve is seen in all three channels. At higher altitudes, the relative brightness of the red channel of Steve appears to increase, which is also

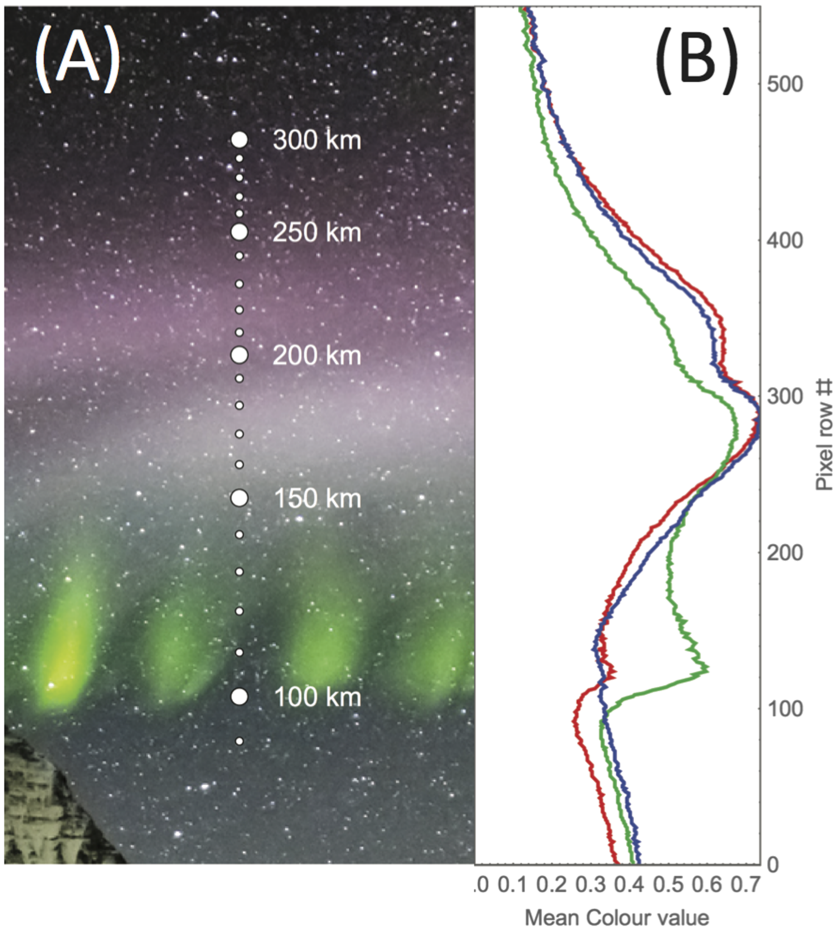

Figure 4. (a) Altitude profile retrieved for Steve and picket fence under the assumption that both phenomena extend along the Earth's magnetic field. The altitude markers are superimposed on a section of Robert Downie's (O1) photograph already shown in Figure 1. (b) Mean red, green, and blue normalized channel brightness for each row of pixels of the image shown in (a). The *y* axis of this figure is scaled to match the pixel rows in (a).

seen in Figure 4a where Steve has a red appearance above roughly 200 km. These qualitative observations should, however, be interpreted with caution as the photographs presented in this study have not been color calibrated for scientific purposes.

4. Discussion and Conclusions

By triangulating observations of Steve and the green picket fence structure from 16 September 2017, we estimate the picket fence to range from roughly 95- to 150-km altitude and Steve to range from roughly 130- to 270-km altitude. Additionally, we find Steve and the picket fence to align with each other along similar magnetic field lines. These altitude estimates are consistent with the picket fence being caused by precipitating electrons, as suggested by Nishimura et al. (2019) and Gillies et al. (2019). This stated that it is currently unclear what source of precipitation is responsible for these green bands spaced roughly 18 km apart, moving steadily westward equatorward of the aurora at between 200 and 300 m/s. It is interesting to note as well that if the two phenomena are exactly field aligned with one another, this has significant consequences on the ionospheric electrodynamics of Steve. Steve appears to be colocated with intense SAID occurring in unusually deep midlatitude density troughs (Archer et al., 2019). Electron precipitation in this region (associated with the picket fence) would significantly enhance the local plasma density, resulting in higher conductivity and lower plasma velocities. As such, the exact relative location of Steve and the picket fence is a significant detail that should be determined precisely in future studies.

Steve is largely above the picket fence and is located in the lower *F* region. Gillies et al. (2019) describe known sources of airglow, which typically peak in brightness around 100-km altitude, as potentially responsible for

the visual continuum of Steve. If these chemiluminescent reactions (such as those presented by ; Evans et al., 2010, or ; Hedin et al., 2012) are responsible for the optical signatures of Steve presented in this study, they are much brighter than typically reported and are occurring well above their typical altitude range. Clearly, there is unforeseen chemistry at work here. Large upflows like those reported by Nishimura et al. (2019), which are a known signature of SAID (Anderson et al., 1991), may also play a significant role in unusual ionospheric conditions resulting in Steve. We presumably need to find a chemiluminescent reaction that can create a continuum in the visual part of the spectrum ranging, this between 130- and 270-km altitude.

Acknowledgments
Unaltered digital copies of all images used in this study are available online (doi:10.5683/SP2/1VPEFE). William Archer was supported by grants from the European Space Agency and the Natural Sciences and Engineering Council of Canada. We would like to thank the Alberta Aurora Chasers (AAC) for facilitating this research. It is through the AAC that we identified a suitable event for study and were able to contact the photographers. We hope to continue working with this enthusiastic community in the future.

References

Anderson, P. C., Heelis, R. A., & Hanson, W. B. (1991). The ionospheric signatures of rapid subauroral ion drifts. *Journal of Geophysical Research*, *96*, 5785. https://doi.org/10.1029/90JA02651

Archer, W. E., Gallardo-Lacourt, B., Perry, G., St-Maurice, J.-P., Buchert, S. C., & Donovan, E. (2019). Steve: The optical signature of intense subauroral ion drifts. *Geophysical Research Letters*, *46*, 6279–6286. https://doi.org/10.1029/2019GL082687

Cole, K. D. (1965). Stable auroral red arcs, sinks for energy of Dst main phase. *Journal of Geophysical Research*, *70*, 1689–1706. https://doi.org/10.1029/JZ070i007p01689

Evans, W. F. J., Gattinger, R. L., Slanger, T. G., Saran, D. V., Degenstein, D. A., & Llewellyn, E. J. (2010). Discovery of the FeO orange bands in the terrestrial night airglow spectrum obtained with OSIRIS on the Odin spacecraft. *Geophysical Research Letters*, *37*, L22105. https://doi.org/10.1029/2010GL045310

Gallardo-Lacourt, B., Liang, J., Nishimura, Y., & Donovan, E. (2018). On the origin of STEVE: Particle precipitation or ionospheric skyglow? *Geophysical Research Letters*, *45*, 7968–7973. https://doi.org/10.1029/2018GL078509

Gallardo-Lacourt, B., Nishimura, Y., Donovan, E., Gillies, D. M., Perry, G. W., Archer, W. E., et al. (2018). A statistical analysis of STEVE. *Journal of Geophysical Research: Space Physics*, *123*, 9893–9905. https://doi.org/10.1029/2018JA025368

Gillies, D. M., Knudsen, D., Donovan, E., Jackel, B., Gillies, R., & Spanswick, E. (2017). Identifying the 630 nm auroral arc emission height: A comparison of the triangulation, FAC profile, and electron density methods. *Journal of Geophysical Research: Space Physics*, *122*, 8181–8197. https://doi.org/10.1002/2016JA023758

Gillies, D. M., Knudsen, D., Donovan, E., Jackel, B., Gillies, R., & Spanswick, E. (2019). First observations from the TREx spectrograph: The optical spectrum of STEVE and the Picket Fence phenomena. *Geophysical Research Letters*, *46*, 7207–7213. https://doi.org/10.1029/2019GL083272

Hedin, J., Rapp, M., Khaplanov, M., & Stegman, J. (2012). Geophysicae observations of NO in the upper mesosphere and lower thermosphere during ECOMA 2010. *Annales Geophysicae (November)*, *30*, 1611–1621. https://doi.org/10.5194/angeo-30-1611-2012

Hirsch, M. (2016). pymap3d, Boston, MA.

Kozyra, J. U., Valladares, C. E., Carlson, H. C., Buonsanto, M. J., & Slater, D. W. (1990). A theoretical study of the seasonal and solar cycle variations of stable aurora red arcs. *Journal of Geophysical Research*, *95*, 12,219–12,234. https://doi.org/10.1029/JA095iA08p12219

MacDonald, E. A., Donovan, E., Nishimura, Y., Case, N. A., Gillies, D. M., Gallardo-lacourt, B., et al. (2018). New science in plain sight: Citizen scientists lead to the discovery of optical structure in the upper atmosphere. *Science Advances*, *4*(March), 16–21. https://doi.org/10.1126/sciadv.aaq0030

Mathematica (2017). Wolfram Research, Inc., Champaign, IL.

Nishimura, Y., Gallardo-Lacourt, B., Zou, Y., Mishin, E. V., & Knudsen, D. J. (2019). Magnetospheric signatures of STEVE: Implication for the magnetospheric energy source and inter-hemispheric conjugacy. *Geophysical Research Letters*, *46*, 5637–5644. https://doi.org/10.1029/2019GL082460

SkySafari Corp. (2019). Simulation curriculum, Minnetonka, MN.

Weber, E. J., Buchau, J., Moore, J. G., Sharber, J. R., Livingston, R. C., & Reinisch, B. W. (1984). F layer ionization patches in the polar cap. *Journal of Geophysical Research*, *89*, 1683–1694. https://doi.org/10.1029/JA089iA03p01683

Weber, E. J., Klobuchar, J. A., Buchau, J., & Carlson, H. C. (1986). Polar cap F layer patches: Structure and dynamics. *Journal of Geophysical Research*, *91*, 121–129. https://doi.org/10.1029/JA091iA11p12121